ESD-TR-68-307

A METHOD TO DETERMINE AN EFFECTIVE RADIO REFRACTIVITY PROFILE BY DIRECT RADIOMETRIC MEASUREMENTS

Lyall G. Rowlandson

30 January 1968

AEROSPACE INSTRUMENTATION PROGRAM OFFICE
ELECTRONIC SYSTEMS DIVISION
AIR FORCE SYSTEMS COMMAND
UNITED STATES AIR FORCE
L. G. Hanscom Field, Bedford, Massachusetts

(Prepared under Contract No. F19628-68-C-0209 by Syracuse University Research Corporation, Merrill Lane, University Heights, Syracuse, New York.)

LEGAL NOTICE

When U. S. Government drawings, specifications or other data are used for any purpose other than a definitely related government procurement operation, the government thereby incurs no responsibility nor any obligation whatsoever; and the fact that the government may have formulated, furnished, or in any way supplied the said drawings, specifications, or other data is not to be regarded by implication or otherwise as in any manner licensing the holder or any other person or conveying any rights or permission to manufacture, use, or sell any patented invention that may in any way be related thereto.

OTHER NOTICES

Do not return this copy. Retain or destroy.

ESD-TR-68-307

A METHOD TO DETERMINE AN EFFECTIVE RADIO REFRACTIVITY PROFILE BY DIRECT RADIOMETRIC MEASUREMENTS

Lyall G. Rowlandson

30 January 1968

AEROSPACE INSTRUMENTATION PROGRAM OFFICE
ELECTRONIC SYSTEMS DIVISION
AIR FORCE SYSTEMS COMMAND
UNITED STATES AIR FORCE
L. G. Hanscom Field, Bedford, Massachusetts

(Prepared under Contract No. F19628-68-C-0209 by Syracuse University Research Corporation, Merrill Lane, University Heights, Syracuse, New York.)

FOREWORD

This report is prepared for the

Aerospace Instrumentation Program Office
Electronics Systems Division
Air Force Systems Command of the United States Air Force
L. G. Hanscom Field
Bedford, Massachusetts

Air Force Program Monitor - Lt. K. Troup, ESD/ESSIE

Project Number 6684, Task 6684.05

covering research over the period

1968 February 1 to 1968 September 1.

Prepared under Contract No. F19628-68-C-0209 by

Syracuse University Research Corporation
Merrill Lane, University Heights
Syracuse, New York

This report was reviewed and approved by

James Shunk, Captain, USAF
Program Manager for ESD/ESSIE/6684.

ABSTRACT

During late 1964, a joint Canadian and United States Air Force experiment was carried out at Cold Lake, Alberta, Canada, to examine multipath propagation effects on various types of radio signals. A relatively simple, vertical reflection interferometer was used to record the received signal variations from an airborne radio source. Direct meteorological measurements were carried out along the paths of the radio signals within the same time frame. This paper is concerned with the radiometric results which relate the radio signal fading pattern, due to multipath, to effective earth radii values. Using the meteorological measurements independent ray tracing calculations demonstrate that the interferometer provides meaningful measurements of the effective ray path bending under various propagation conditions. Based on these observations the following paper develops a method to generate the effective radio refractivity profile from direct, interferometer radiometric measurements. An analysis of the accuracy requirements indicates that the method is within the state-of-the-art and can be modified in a simple way, using two frequencies, to calculate the effective height of the receiver relative to the reflecting surface. This latter ability is particularly important for measurements over the ocean. The technique appears to provide a direct and simple method to measure effective radio propagation conditions in real-time. For many applications this approach has significant advantages since it reduces the usual requirement to take extensive airborne meteorological measurements.

TABLE OF CONTENTS

LIST OF ILLUSTRATIONS

1. INTRODUCTION

Radio ray propagation conditions are usually determined by direct meteorological measurements through the use of balloon-borne instrumentation and/or instrumented aircraft. This approach has two disadvantages.

In the first case, if the propagation conditions are to be defined in detail the measurements can require the use of several airborne facilities to counteract the effect of spatial and temporal variations. This approach leads to a large amount of data with the usual difficulty in processing them in a useful time period.

Secondly, the effect of small variations of the radio refractivity structure on radio propagation parameters, such as range errors, cannot be determined without additional ray tracing analysis.

The following presentation suggests a method to determine the effective radio refractivity model by direct radio propagation measurements. The concept was generated by results obtained from a comprehensive field experiment wherein a vertical reflection interferometer was used to determine the angle of arrival of radio signals. In the final analysis a comparison was made between the "effective earth radii" calculated from the radio interferometer data and by a separate calculation using direct meteorological measurements together with ray tracing analyses.

The agreement between the comparative data was significantly good and the idea was then germinated as to the possible direct use of radio interferometer data to measure the effective propagation conditions without direct meteorological support. The final projection was to determine if an "effective" radio refractivity profile could be generated using the interferometer earth radii data. The following analyses will demonstrate that this is analytically and technically feasible.

2. THE DETERMINATION OF EFFECTIVE EARTH RADII FROM RADIO INTERFEROMETER MEASUREMENTS

In the reflection interferometer technique the signal from the radio source arrives at the receiving antenna via two paths (Figure 1), i.e., by the "direct ray" (S_1) and by the "reflected ray" (S_2). S_1 and S_2 combine vectorially according to their phase differences and also their relative amplitudes.

The phase difference between the two signals is a function of the path length difference of the two rays in terms of wavelengths (λ) of the transmission frequency and also of the phase change in the reflected ray at the surface. For water and small angles of incidence the phase change on reflection is essentially 180 degrees. Therefore, the two signals will cancel at the receiver when the electrical path length differences are integral multiples of the transmission wavelength. Then the received power will oscillate between a maximum and minimum level given by

$$(1 - \rho)\, P \leq P_r \leq (1 + \rho)\, P \tag{1}$$

where P is the power received along the direct path, S_1, and ρ is the magnitude of the reflection coefficient. As the source moves toward the receiver the signal will be a minimum when the path length difference, ΔR, is

$$\Delta R = n\lambda \tag{2}$$

where $n = 1, 2, 3, \ldots,$ etc.

Figure 2 shows a typical received signal power pattern as the radio source varies in range with respect to the receiver and maintains a constant height from the reflecting surface.

Referring to Figure 3, the electrical ranges $\mathbb{D}$, measured over the direct path, which produce minima (fades) is given by

$$\mathbb{D}\, n \simeq \frac{2h_1' \cdot h_2'}{n\lambda} \tag{3}$$

The true heights of the receiving antenna, h_1, and source, h_2, relative to a curved earth are AA' and BB', respectively. As shown in Appendix I, the range $\mathbb{D}_n$ (Equation (3)) can be determined in terms of h_1, h_2, and the earth radius, A.

A3412

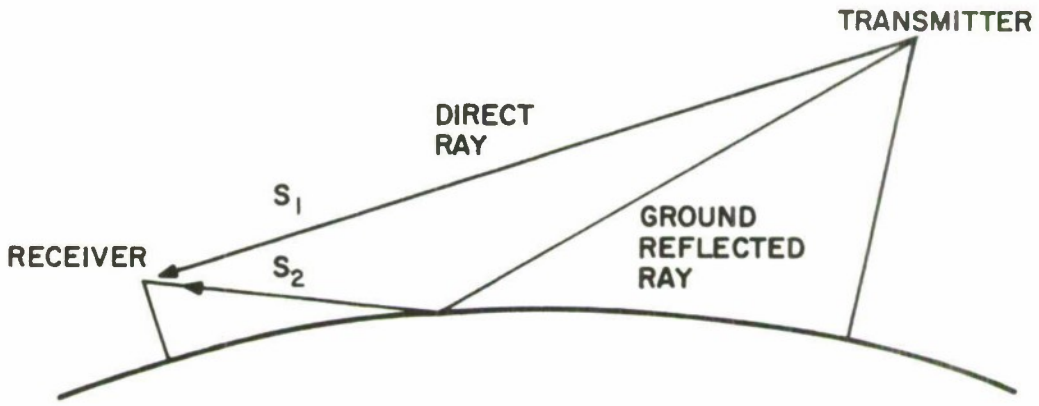

FIGURE 1 VERTICAL INTERFEROMETER STRAIGHT RAY GEOMETRY

A3413

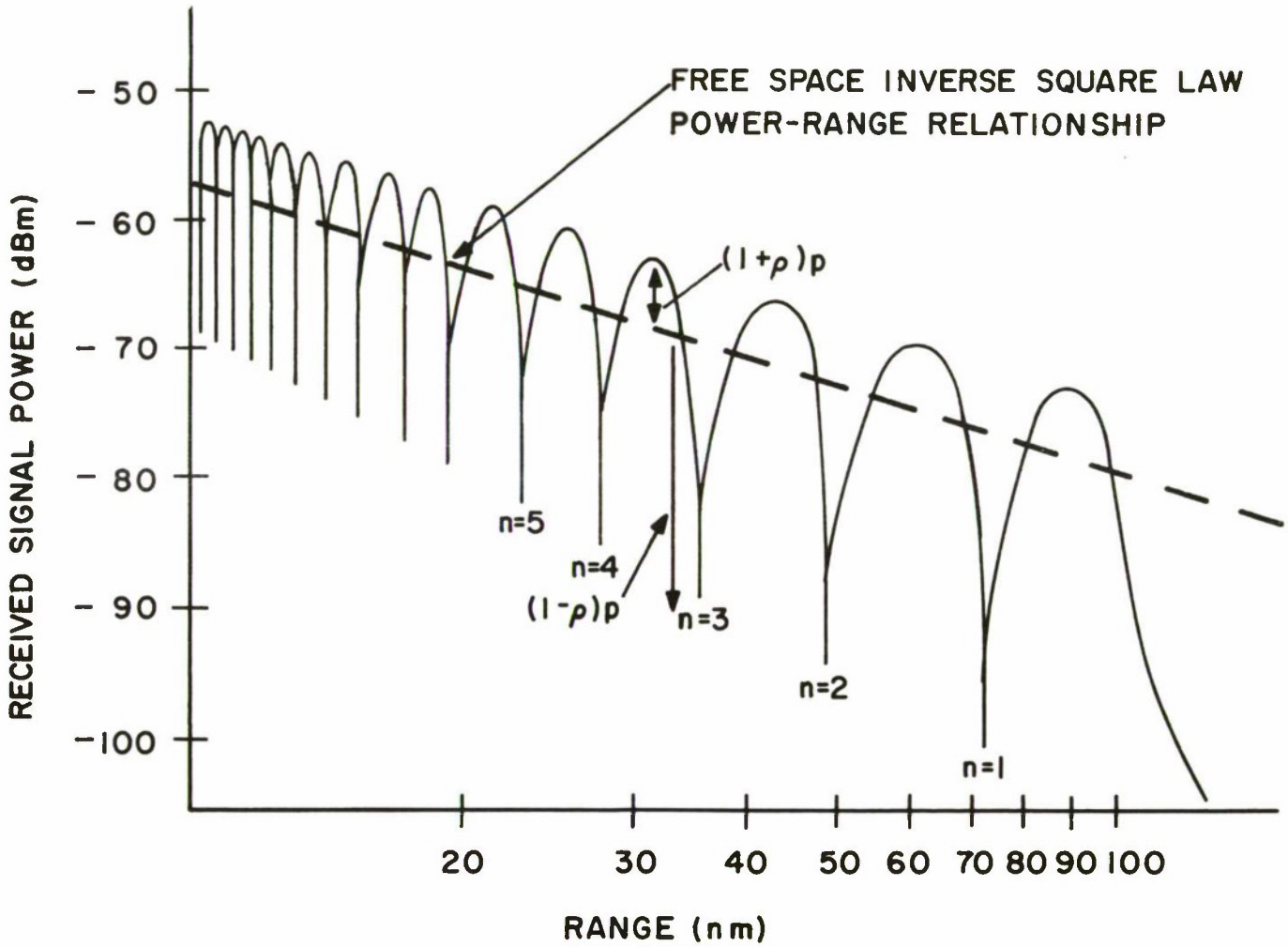

FIGURE 2 VERTICAL INTERFEROMETER INTERFERENCE PATTERN

A3422

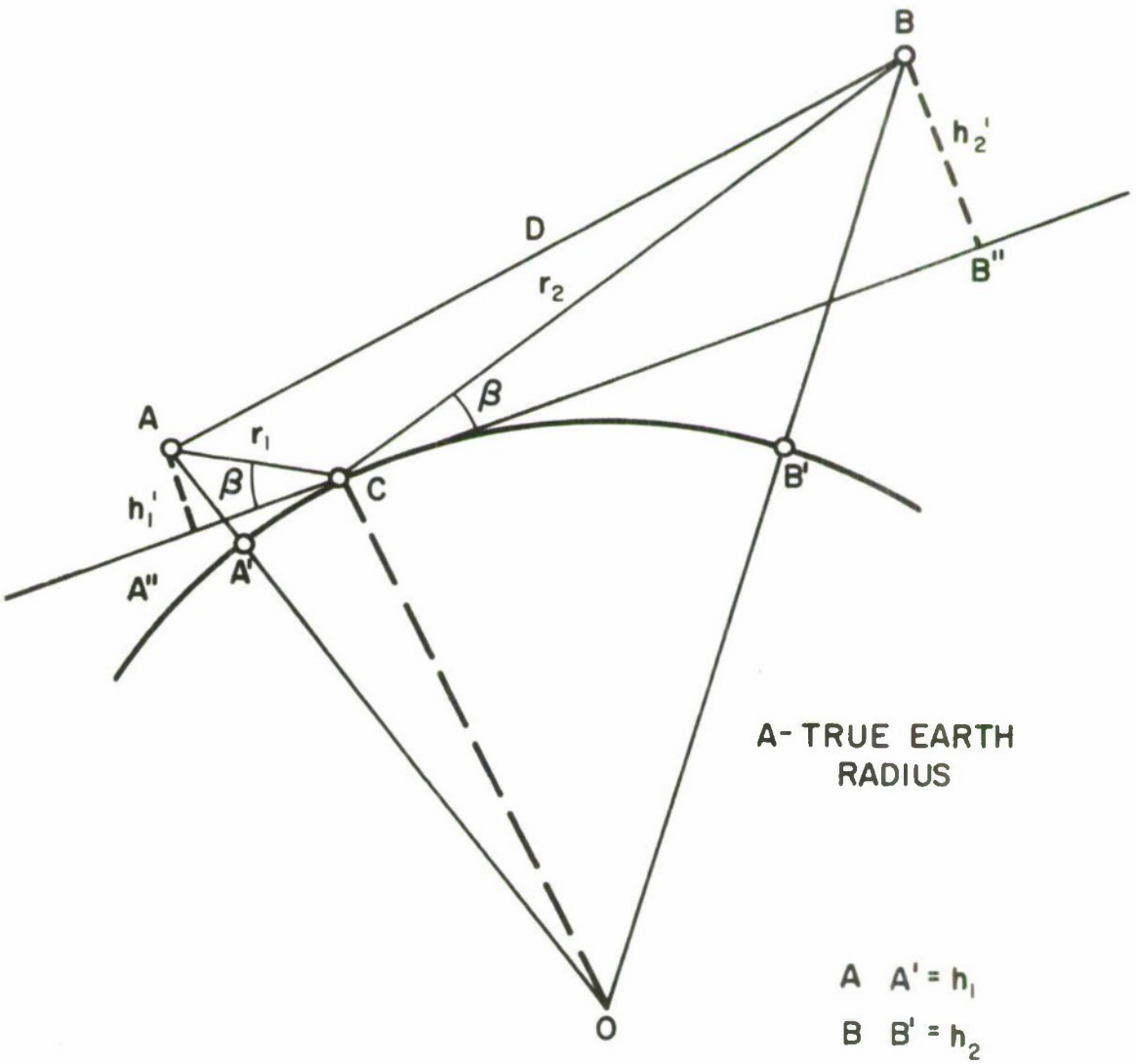

FIGURE 3 GEOMETRY OF FLAT EARTH APPROXIMATION

In practice the rays do not travel in straight lines, however, it was shown by Schelleng, Burrows and Ferrel[1] that by increasing the earth radius to some value, Ae, the curved path geometry can be represented by straight rays, preserving the initial elevation angle of the ray, θ_o, the electrical path range, R, and the height of the source h_2, relative to this new earth surface.

The new "effective earth radius", Ae, is calculated from

$$Ae \simeq \frac{A\, n_o}{n_o + \frac{A}{10^6}\, dN/dh \cdot \cos\theta} \qquad (4)$$

where A is the true earth radius

n_o is a representative value for the surface index of refraction and may be considered to be unity for all practical purposes

dN/dh is the effective gradient of radio refractivity with height where $n = 1 + \frac{N}{10^6}$ and

θ is the local elevation angle of the ray.

In general, the vertical index gradient is not independent of height, in which case Ae would have little analytical usefulness. However, for the moment, let an equivalent effective earth radius Ae be defined to satisfy a particular propagation condition observed from the interferometer results.

Referring to Figure 1 and Equation (3), at a particular time when a fade occurs there is only one value for the earth radius which satisfies the measurement of Δn, h_1' and h_2' to produce the n^{th} fade. Therefore, at each fade condition the geometrical measurements will generate a unique value for Ae which will generally be different from fade-to-fade. The only time the values for Ae could be constant is if one value for Ae can be found which satisfies the geometry for all ranges and initial elevation angles. This situation occurs only if the vertical gradient dN/dh is everywhere a constant, a condition not generally representative in reality, and where cos θ is taken as unity for propagation at small elevation angles (Equation (4)).

3. A COMPARISON OF INTERFEROMETER AND RAY TRACING CALCULATIONS OF THE EQUIVALENT EFFECTIVE EARTH'S RADII

A total of eighty pattern measurements was carried out at the Royal Canadian Air Force, Primrose Lake Evaluation Range, Cold Lake, Alberta, Canada.[2] The receiving site, using a wide-angle microwave antenna, was located on a hill overlooking a large fresh water lake. The radio source was carried in an aircraft at constant altitude (as well as could be flown) with theodolite cameras and radar altimeter recordings used for the final accurate height determinations. The electrical length of the direct path between the receiver and the aircraft was measured by a short pulse radar and time interval electronics system located at the receiving site.

Independent radio refractivity measurements were made using an instrumented aircraft together with periodic radiosonde soundings during the time the radio experiment was being conducted. The refractivity data were then used in a ray tracing analysis to determine the angles of arrival and electrical path lengths corresponding to the position of the signal source aircraft for each radio fade condition. The ray tracing results were then used to further calculate "equivalent effective earth radii" which would satisfy the initial elevation angles and ranges, corresponding to the geometry at each fade.

The radio propagation and independent ray tracing results for Ae were then compared for all the tests undertaken.

Figure 4 shows the average differences between the results, together with the standard deviation, plotted against the transmitter range R. The estimated error in the interferometer results is shown by the dashed curve (Appendix II). The errors increase at short ranges due to the fact that the signal source height and range errors become more significant.

One objective in the experiment was to relate the radiometric and ray tracing calculations of the equivalent effective earth radii, Ae, to within 200 nm. On the average these results were nearly achieved and to do this required a high degree of accuracy such as signal source height, h_2, within ± 25 feet, receiver height, h_1, within ± 0.05 feet, signal source range, R, within ± 100 feet and a wavelength determination, λ, within ± 0.001 feet. During the experiment both vertical and horizontal polarizations were available for use at L- and S-Bands.

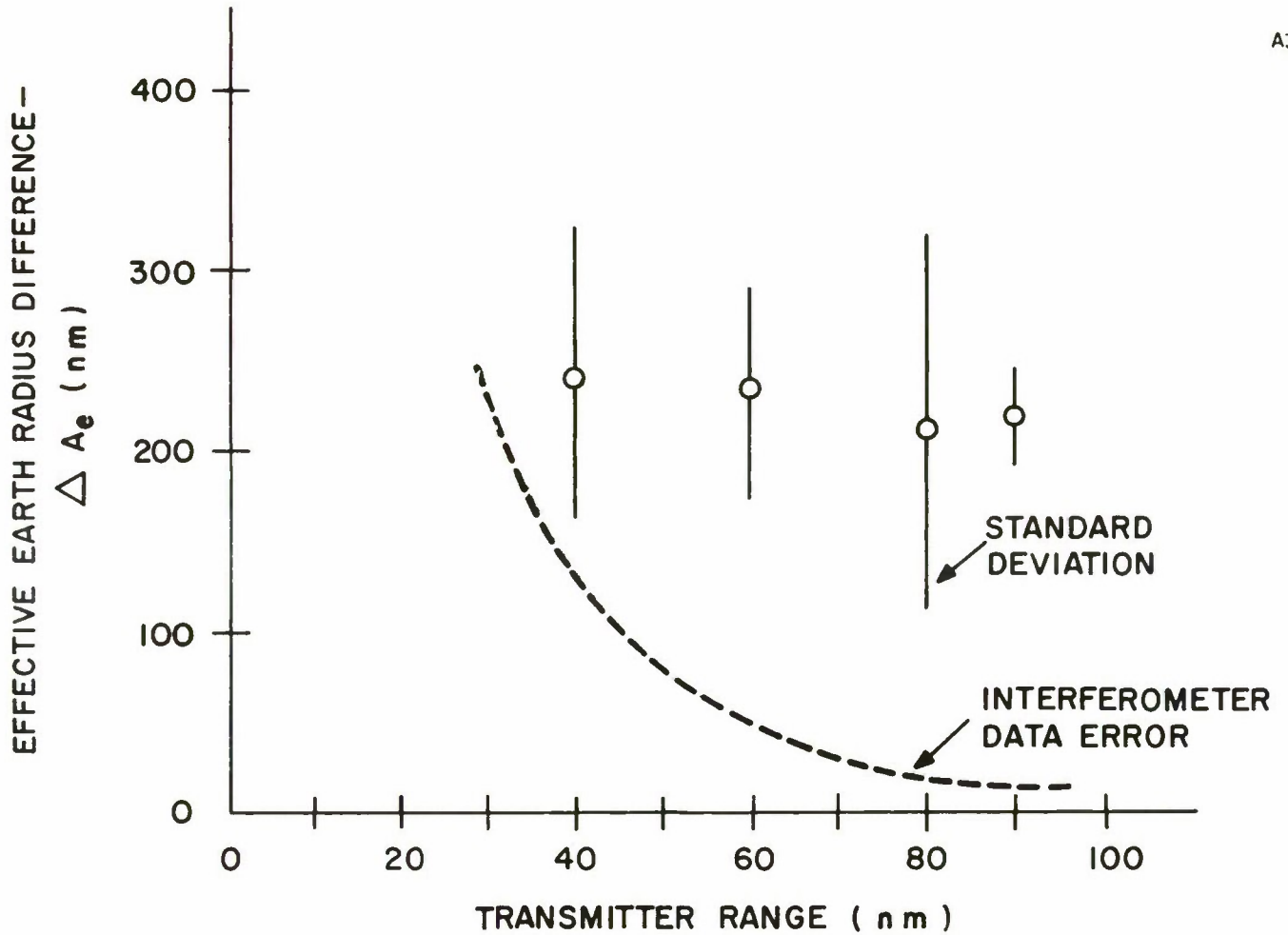

IA-19,644

FIGURE 4 EFFECTIVE EARTH RADIUS DIFFERENCE (nm) BETWEEN RAY-TRACING AND INTERFEROMETER RESULTS VERSUS RANGE

4. A COMPARISON OF EFFECTIVE PROPAGATION CONDITIONS WITH RADIOMETRIC MEASUREMENTS

Any one set of earth radii values generate a corresponding set of refraction gradients, dN/dh, as shown from Equation (4). Larger values of earth radii represent correspondingly larger values for the magnitudes of the gradients.

Figure 5 is a plot of the received radio signal levels for a particular flight. Figure 6 shows the radiometric calculations for Ae, obtained for each fade condition plotted against the radio source range from the receiving site. Two sets of data are shown corresponding to inbound (Figure 5) and outbound flights. Within thirty miles range the accuracy decreases due to the effect of range and height errors, as previously discussed. Beyond thirty miles the magnitudes of the earth radii values, Ae, are seen to be essentially constant, which suggests that a constant gradient refractivity profile represents the propagation conditions. Figure 7 shows the radio refractivity profile measured with a radiosonde from a launch point approximately twenty-five miles from the receiving site and in the direction of the aircraft flight path. As indicated the refractivity gradient is essentially constant.

Figure 8 shows a different situation, where the radiometric, Ae, values are seen to increase with range, which, therefore, suggests that the gradient is increasing in magnitude. Figure 9 shows the measured refractivity profile and it is apparent that the gradient is increasing at the lower levels. As the signal source range increases the ray passes through more of the lower atmosphere, where the larger gradient would become more effective. Therefore, the radiometric data and the radio refractivity profile characteristics show a consistent behavior.

In general, the radiometric and propagation data show surprisingly good correspondence in terms of the relative variations of earth radii and the effective refractivity gradients with height. Aircraft meteorological measurements were similar to the radiosonde data with the exception that greater fine-structure could be resolved. This latter information is not particularly important to the average conditions under discussion herein.

The remaining problem is how to exploit the radiometric measurement technique to define the effective propagation conditions. Several possible configurations are discussed in the following sections.

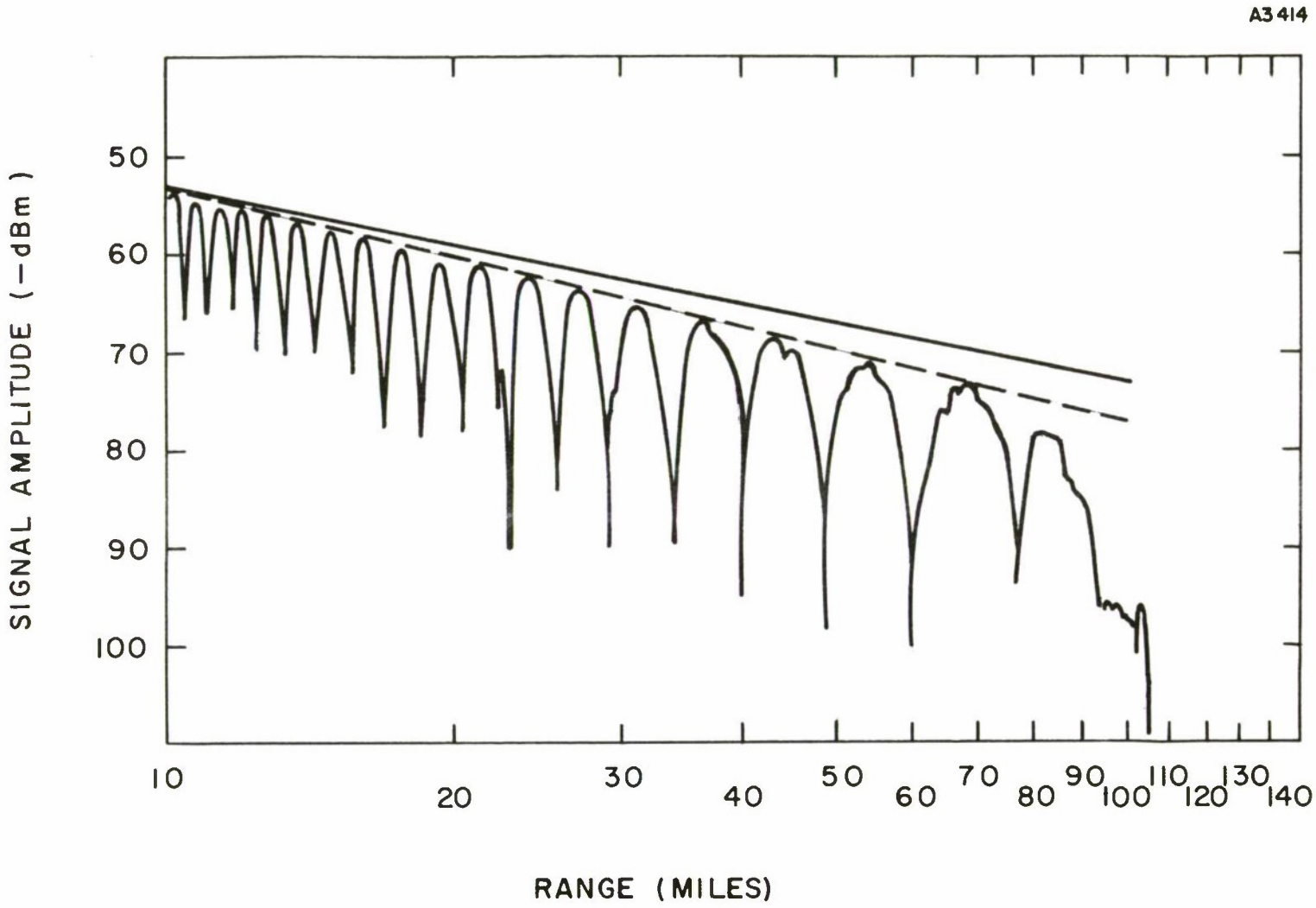

FIGURE 5 SIGNAL AMPLITUDE VERSUS RANGE

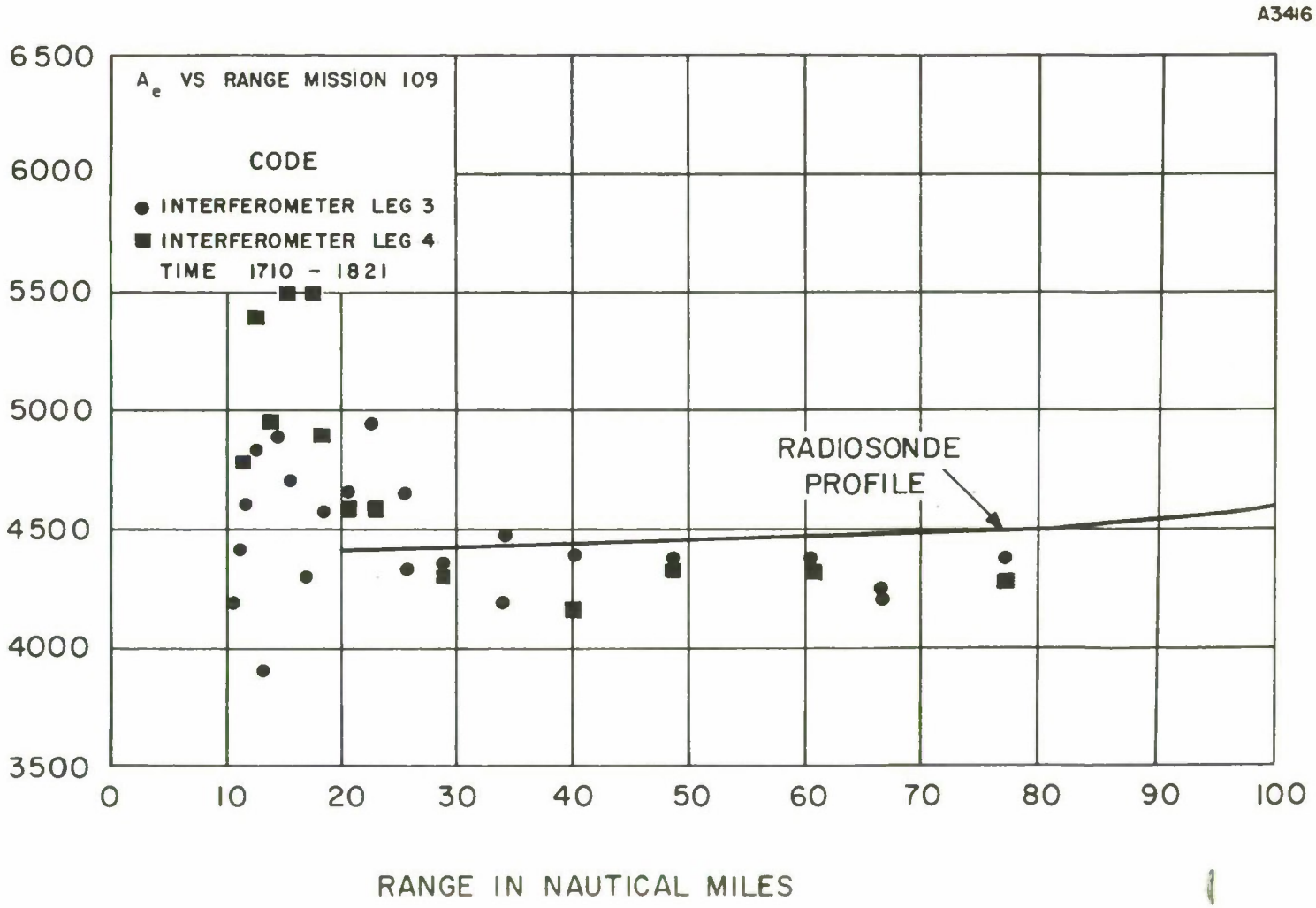

FIGURE 6 EFFECTIVE EARTH RADII VALUES VERSUS RANGE

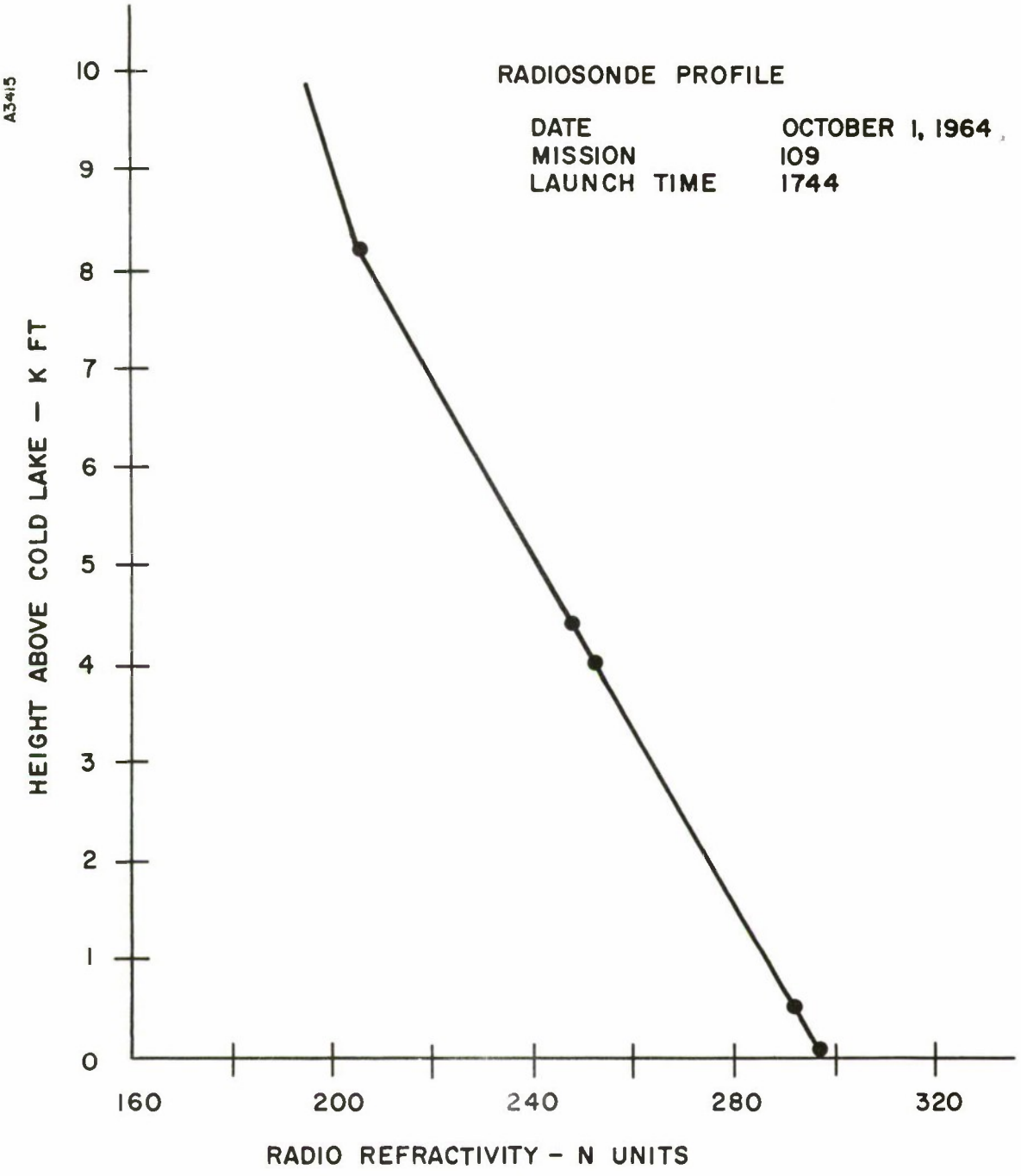

FIGURE 7 RADIO REFRACTIVITY PROFILE

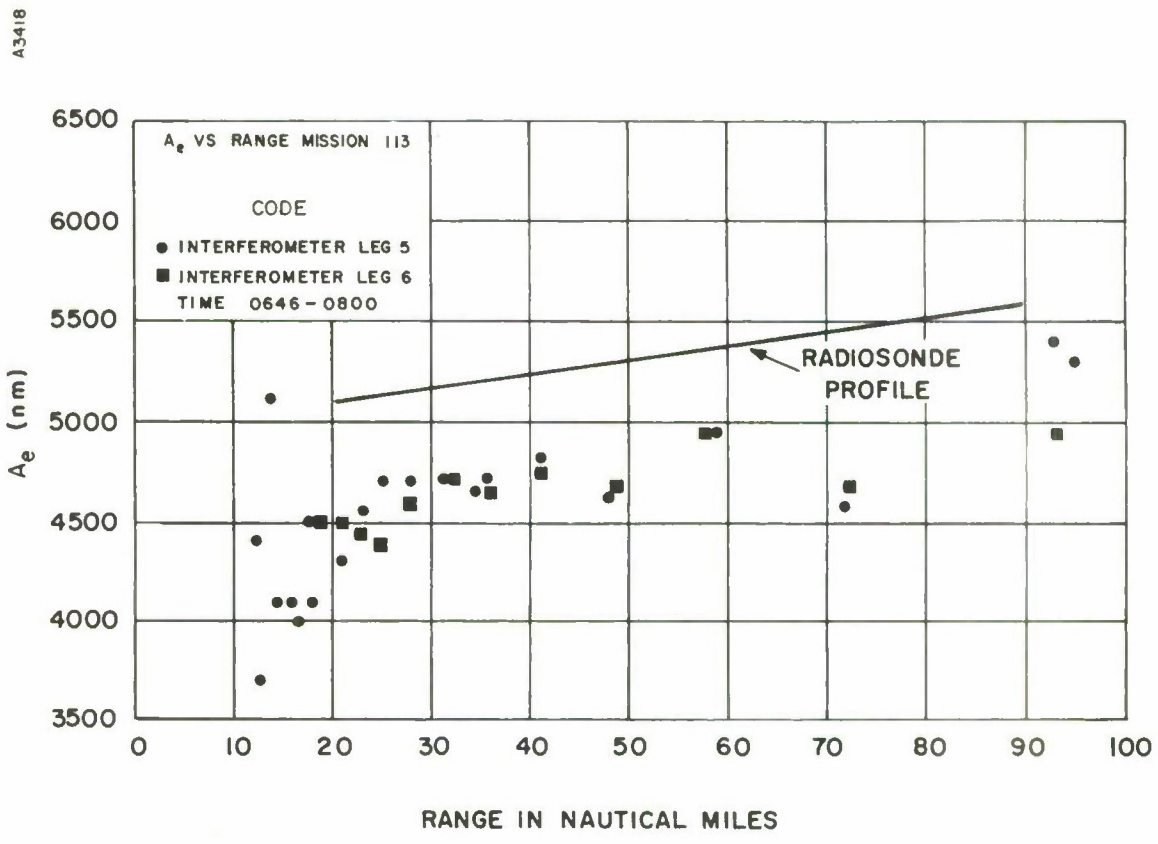

FIGURE 8 EFFECTIVE EARTH RADII VALUES VERSUS RANGE

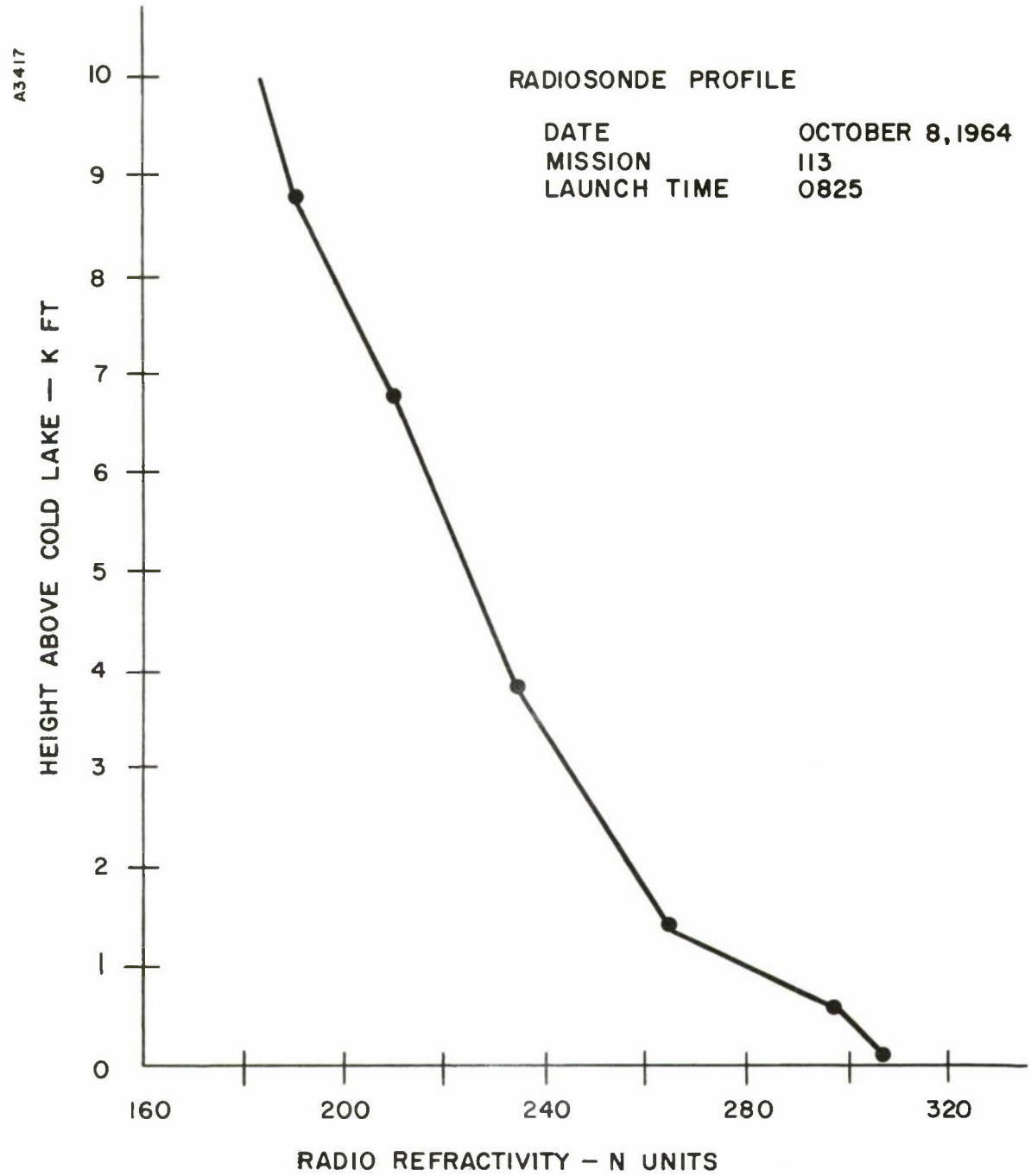

FIGURE 9 RADIO REFRACTIVITY PROFILE

5. A DISCUSSION OF METHODS TO USE RADIOMETRIC MEASUREMENTS TO DETERMINE PROPAGATION CONDITIONS

Any determination of propagation conditions is, in the first place, restricted to the maximum height of the signal source aircraft. However, since most of the non-standard variations in the refractivity profile occur below 15,000 feet the experiment can be limited in height, with radiosonde measurements used above this level to define the average, spherically stratified conditions.

In order to reduce the effect of range measurement errors and the cos θ factor (Equation (4)), the source should be located at long ranges but within the radar horizon. The larger the wavelength the greater will be the separation between fades. However, the number of fades will be correspondingly reduced which limits the precise definition of the propagation conditions.

As the aircraft range changes, and with the height maintained constant, the degree of ray path curvature depends upon the initial elevation angle which, in this case, is the angle of arrival. In order to obtain a meaningful measurement of the propagation conditions it would be convenient to generate the values of effective earth radii as a function of radio source height rather than in terms of range.

These considerations suggest an experiment where the radio source is constrained at some desirable range and rises from a point below the radio horizon to some maximum altitude.

As the source rises above the radio horizon the first order fade (n = 1) can be determined and all subsequent order fades then accountable.

From Equation (3) fades occur whenever

$$h_2' \simeq \frac{nR\lambda}{2h_1'} \tag{5}$$

and $n = 1, 2, 3, \ldots,$ etc.

Replacing h_2' and h_1' by their corresponding values of h_1 and h_2 (Appendix I), gives

$$h_2 \simeq \frac{(R - r_1)^2}{2Ae} + \frac{n\lambda R}{2\left(h_1 - \frac{r_1^2}{2Ae}\right)} \tag{6}$$

and $$r_1 \simeq \frac{(R - r_1)\left(h_1 - \frac{r_1^2}{2Ae}\right)}{h_2 - \frac{(R - r_1)^2}{2Ae}} \qquad (7)$$

which for a particular value of n, λ, R, h_1, and h_2, generates an earth radius Ae.

In the Cold Lake analyses, equations of this kind were solved using a computer due to their complexity. One may obtain an estimate of the variation of received signal with height using Equation (5) and making the tacit assumption that h_1' and h_2' are sufficiently close to h_1 and h_2 to let

$$h_2 \simeq \frac{nR\lambda}{2h_1} \qquad (8)$$

For example, with

$R = 100$ km
$\lambda = 1$ meter
$h_1 = 50$ meters

the fades will occur for source heights of 1000 meter intervals.

With the source at 1000 meters, Equation (8) shows that the aircraft range, if variable, would produce a first order fade at 200 km, second fade at 100 km and a third fade at 66 km. At greater source heights the range variations required to produce range dependent fades will require even greater range changes. Therefore, it would be relatively easy to produce a height-dependent fade pattern without placing severe constraints on the permissible aircraft range variations. The height intervals which produce fade data can be decreased, of course, by raising the receiver height or by decreasing the wavelength. However, these changes will affect the permissible variation of range R and may not be acceptable in practice.

The remaining problem is to use the recorded and calculated data to determine an effective refractivity profile. Referring to Figure 10, the following procedure could be attempted. The source rises above the radio horizon producing the first fade (n = 1) at which time the range R, and aircraft height, $(h_2)_{01}$ is recorded. The solution of the geometry, (Equations (6) and (7)), gives a particular value for the effective earth radius, Ae. From Equation (4), with n_0 and cos θ taken as unity an effective gradient $(dN/dh)_{01}$ is determined. This gradient will then represent the average propagation

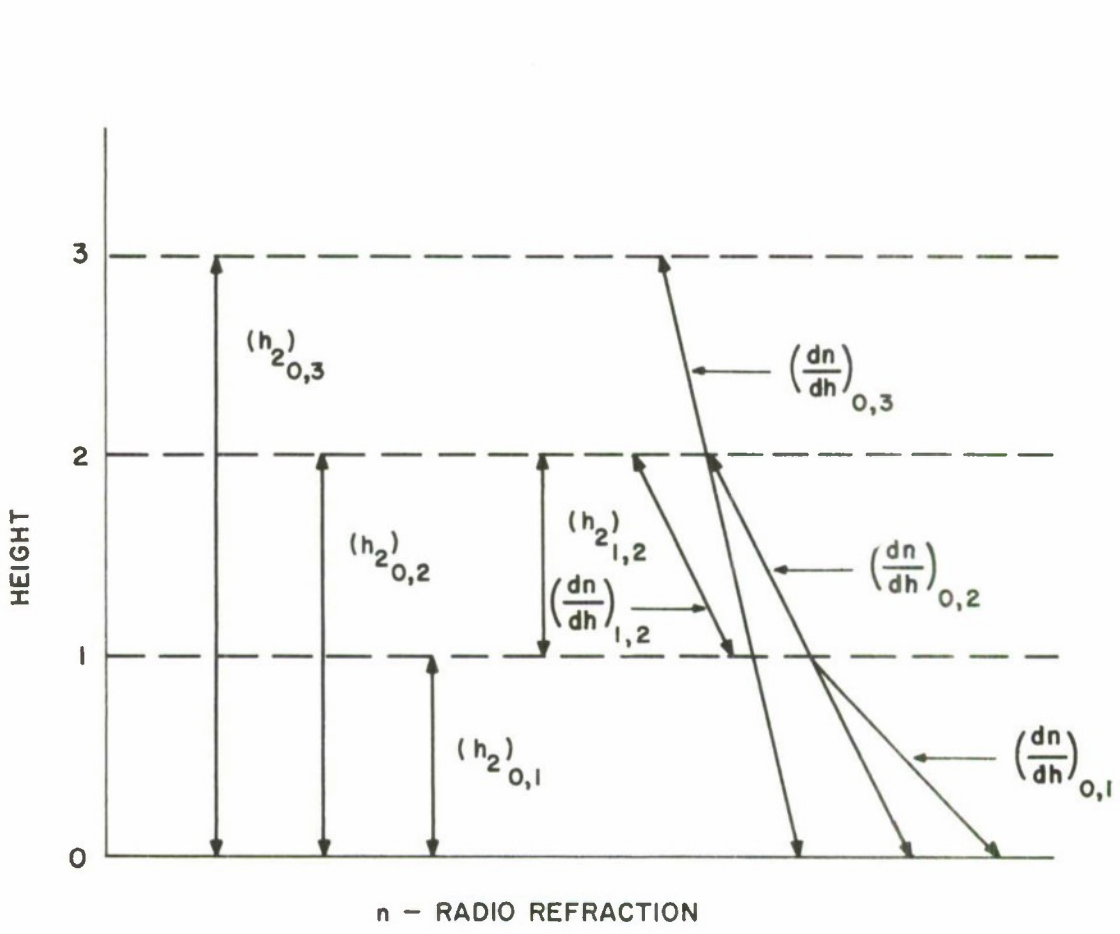

FIGURE 10 PIECEWISE CONSTRUCTION OF THE RADIO REFRACTIVITY PROFILE

condition over this first height interval $(h_s)_{01}$ and over the horizontal extent of the range R. When the second fade occurs (n = 2), in the same way the average effective gradient $(dN/dh)_{02}$ is found which extends over the height interval $(h_s)_{02}$.

It is readily seen that

$$\left(\frac{dN}{dh}\right)_{02} (h_s)_{02} \simeq \left(\frac{dN}{dh}\right)_{01} (h_s)_{01} + \left(\frac{dN}{dh}\right)_{12} (h_s)_{12} \ldots \tag{9}$$

from which the average effective gradient over the interval $(h_s)_{12}$ can be determined. The procedure is continued with each fade in height until the overall vertical gradient profile is determined in height sections. Also, the relative values for the radio refractivity can then be determined from a knowledge of the individual gradients and the magnitudes of the respective height intervals. In theory, a vertical refractivity profile can then be constructed and made to fit the appropriate refractivity readings obtained at higher elevations with the radiosonde data. Since the surface refractive index, n_0, is probably quite variable it would be difficult to select a suitable n_0 from which to generate the absolute profile. For this reason it is more meaningful to tie the profile to measurements at the higher levels. These high-level measurements can be obtained from a radiosonde launched anywhere within the general area.

6. THE SENSITIVITY OF THE RADIOMETRIC MEASUREMENTS TO CHANGES IN THE REFRACTIVITY GRADIENTS

The results obtained in the Cold Lake experiment demonstrated that there was a general tendency for the effective earth radii values, Ae, to vary in accordance with changes in the propagation conditions. It is useful to analyze the expected variations as a function of gradient changes in order to determine whether or not sensible data may be obtained within limits imposed by experimental errors.

Assuming that the same accuracies can be obtained as in the Cold Lake experiment (Section 3), the error in the effective earth radii calculations will be set at ±200 nautical miles.

From Equation (4), with cos θ set equal to unity, then

$$\frac{\delta(Ae)}{Ae} \simeq - \frac{Ae}{10^6} \cdot \delta\left(\frac{dN}{dh}\right) \tag{10}$$

where N is the radio refractivity
Ae is the effective earth radius.

Considering standard conditions, then setting Ae to be 4600 nm, (i.e., 8500 km) then

$$\delta(dN/dh) = \pm 5N/km \tag{11}$$

For experimental conditions outlined in Section 5, this result indicates that the gradient calculation over the first kilometer height interval could not be determined to better than ±5N/km. Comparing with an exponential reference atmosphere,[3] where the initial gradient is about 40 N/km near sea level, it is apparent that the measurement would be in error by at least ±12 percent.

At the second height interval the average gradient error would again be about 12 percent. Referring to Equation (9) the gradient in the interval $(h_2)_{12}$ would be affected by the combined errors, and so on, with the cumulative errors increasing with height. Since there is no bias toward the sign of the errors the final accumulated error over five fade conditions would not be expected to be 60 percent.

7. SOME COMMENTS ON THE ERROR MAGNITUDES AND METHODS TO REDUCE THEM

From the error analysis equations presented in Appendix II, the Cold Lake data clearly show that the inability to determine the signal source height contributed to most of the error.

The development of radar altimetry provides a present day capability to measure the height above a smooth water surface to within a few feet. If the radar is placed on a stabilized mount to ensure that the range measurement is in the vertical an experiment could be conducted without imposing severe flight requirements on the aircraft. The effect of sea-surface roughness should average out since the radar antenna pattern will encompass a significantly large area on the sea surface.

With a receiver height h_1 of 50 meters, for example, the reflection area or first Fresnel Zone will be very large and located several miles from the shore line. This has two advantages in that surface roughness is averaged out and the effect of local upwelling of the water, near the shore line, is reduced.

The difficult problem is to determine the height, h_1, of the receiver, relative to the reflection area. One method to derive this effective height would be to transmit two signal frequencies from the aircraft and to compare the heights at which the first order fades occur for the individual frequencies.

Then, using the Equations (6) and (7) the first order fades occur where

$$(h_2)_{\lambda_1} = f(R_1, \lambda_1, h_1, Ae) \quad (12)$$

$$(h_2)_{\lambda_2} = f(R_2, \lambda_2, h_1, Ae) \quad (13)$$

where the difference between λ_1 and λ_2 is only large enough to separate the individual signals at the receiver. If the fades occur within a small variation of range, R, and height, h_2, then Ae can be considered to be the same for both conditions. The effective receiver height, h_1, can then be found.

There may be some advantage to continue the use of two frequencies since several values for h_1 can then be calculated and a more meaningful average value determined. Furthermore, the use of two frequencies provides a second measure of the refractivity profile at different heights than the values obtained with the first frequency. In the event of antenna shading by the aircraft the second set of data provides additional reliability in the experiment.

However, from the error analysis Equation (3) (Appendix II) assuming two wavelengths are used, and with R and Ae essentially the same for both fade conditions at λ_1 and λ_2 then

$$h_1 \simeq \frac{R\,(\lambda_2 - \lambda_1)}{2\,((h_2)_2 - (h_2)_1)} \tag{14}$$

For a range of 100 km, a wavelength separation of 0.1 meters at a mean wavelength of 1 meter, then estimating from Equation (8) the fades occur at 1000 and 1100 meters. Assuming a range measurement error of ±30 meters, a wavelength measurement error of ±0.0003 meters and a height measurement error of ±2 meters, then the errors in h_1 from Equation (14) are

a. 0.015 m. due to the range uncertainty,
b. 0.3 m. due to the wavelength uncertainty,
c. 1.0 m. due to the aircraft height uncertainty,

or an accumulated error of about 1.3 meters, largely due to the aircraft height error.

From Equation (11) on Appendix II, this leads to an estimate of the effective earth radius error due to h_1, where

$$\left(\frac{\delta Ae}{Ae}\right)_{h_1} = \left(1 - \frac{2h_2Ae}{R^2}\right)\left(\frac{\delta h_1}{h_1}\right) \tag{15}$$
$$= (0.7)\,(\delta h_1/h_1)$$
$$= (0.7)\,(1/50) \times 100 = 1.8\% \text{ error}$$

This is an acceptable error and it is seen that the effect of the receiving height uncertainty is reduced under long range propagation conditions and by placing the receiver at a significant height above the reflecting surface.

From the error analysis, Equations (10), (11), (12), (13), (Appendix II), the error contributions to the determination of the effective earth radii are then

a. 0.11% due to a 30 meter range error.
b. 1.8% due to a 1.3 meter receiving antenna height error.
c. 0.34% due to a 2 meter aircraft height error.
d. 0.051% due to a 0.0003 meter wavelength error.

That is, a total error of 2.3%

From Equation (10) the gradient error is then 0.27% which for the exponential reference atmosphere represents a gradient error of about ±0.11 N units per km. This accuracy is certainly adequate.

It is significant to note that the bulk of this error is contributed by the indeterminacy in the receiver height relative to the effective reflecting surface. Over a smooth water surface, such as an inland lake, the receiver height can be determined very accurately through the use of standard surveying methods. However, over the ocean, the height would probably have to be indirectly determined such as with the two frequency method in which case the receiver height error is expected to remain the more difficult parameter to calculate.

From the error analysis Equation (11) (Appendix II) it is seen that

$$\left(\frac{\delta Ae}{Ae}\right)_{h_1} \simeq \left(1 - \frac{2h_2 Ae}{R^2}\right)\left(\frac{\delta h_1}{h_1}\right) \tag{16}$$

At the first order fade, (n = 1), h_2 equals 1 km, range R_1 equals 100 km, then

$$\frac{2h_2 Ae}{R^2} > 1$$

Therefore, as successive data are obtained at greater heights, the receiver height error δh_1, will become larger. Therefore, it is of particular importance that h_1 be determined by any possible method which will improve its accuracy.

Furthermore, the gradient decreases with height (based upon an exponential model) in which case the above error, δh_1, becomes even more significant. Around 5 km, in height a typical refractivity variation is 20 N units per kilometer.

From the error analysis and using Equation (15) the accumulated error after five fades is readily shown to be about 1.4% in the effective gradient determination for the 5 kilometer height section $(h_2)_{05}$. Similar to the method illustrated by Equation (9) the error in the gradient determination over the height interval $(h_2)_{45}$ is then given by the accumulated errors in (dN/dh) over each section and weighted by the factor, h_2, as shown by Equation (16). The accumulated error is readily shown to be about 4%, which is acceptable.

8. SUMMARY AND CONCLUSIONS

The vertical reflection interferometer experiment conducted at Cold Lake demonstrated that radiometric measurements could provide values of the effective earth radii which compare favorably with independent ray tracing analyses.

These results lead to a procedure which could generate the effective vertical radio refractivity profile by a modified experimental procedure. In this case a radio source is carried in height at a long range from the receiver such as to generate a multipath fading pattern which is essentially only height dependent. At the time of each ordered fade, the solution of the geometry generates a particular earth radius value, Ae, which can, in turn, be used to determine an effective refractivity gradient over the corresponding height interval. Successive calculations at each fade condition lead to a piecewise construction of the overall refractivity profile.

In order to improve the experimental accuracy the signal source height relative to the reflecting surface should be determined with the most accurate radar altimeter equipment. A second difficulty which would be experienced in practice is to determine the effective height of the receiving antenna relative to the reflecting surface. It is shown that it can be accomplished by observing the relative fading patterns generated by using two simultaneous frequencies. In fact, under long range conditions and with a receiver placed well above the reflecting surface, the errors in this calculation would be acceptable.

The effects of anomalous propagation conditions were not considered since it is apparent that the experiment would break down should either the direct or reflected signal be removed.

APPENDIX I

THE "EFFECTIVE EARTH RADIUS" CONCEPT

THE "EFFECTIVE EARTH RADIUS" CONCEPT

Referring to Figure 11, a receiver, 'A', at height h_1', will receive signals along two paths from a transmitter, 'F', at height h_2'. The first is the direct path F to A, and assuming that the surface is highly reflective, the second path is FGA. As the transmitter moves in range, the signals combine at the receiver to produce minima and maxima amplitude variations. For a water surface and with small grazing angle, β, the phase of the reflected signal is changed by 180 degrees, i.e., π radians. The first fade inside the radio horizon is given the order n = 1 and it occurs at a corresponding transmitter range D_1. As the transmitter moves towards the receiver, each fade condition (minimum received signal) occurs for ranges given by

$$D_n \simeq \frac{2h_1' \cdot h_2'}{n\lambda} \qquad \text{(I-1)}$$

where n = 1, 2, 3, ..., etc.
λ = the radio signal wavelength.

In the real situation, of course, the reflector becomes the surface of a spherical earth. As shown in Figure 12, the true heights of the receiver and the transmitter over the spherical surface are AA' and BB', respectively. If a plane is passed through the reflection point C, Equation (I-1) can be used to determine the fade dependence upon range if h_1' and h_2' are expressed in terms of h_1 and h_2, respectively.

From triangle BCO,

$$\sin \beta = \frac{(A + h_2)^2 - A^2 - r_2^2}{2 A r_2} \qquad \text{(I-2)}$$

also from triangle BCB"

$$h_2' - r_2 \sin \beta \qquad \text{(I-3)}$$

Substituting for sin β into Equation (I-3) and simplifying gives

$$h_2' = h_2 + \frac{h_2^2 - r_2^2}{2A} \qquad \text{(I-4)}$$

Over the range of experimental interest r_2 will be very much greater than h_2

A3421

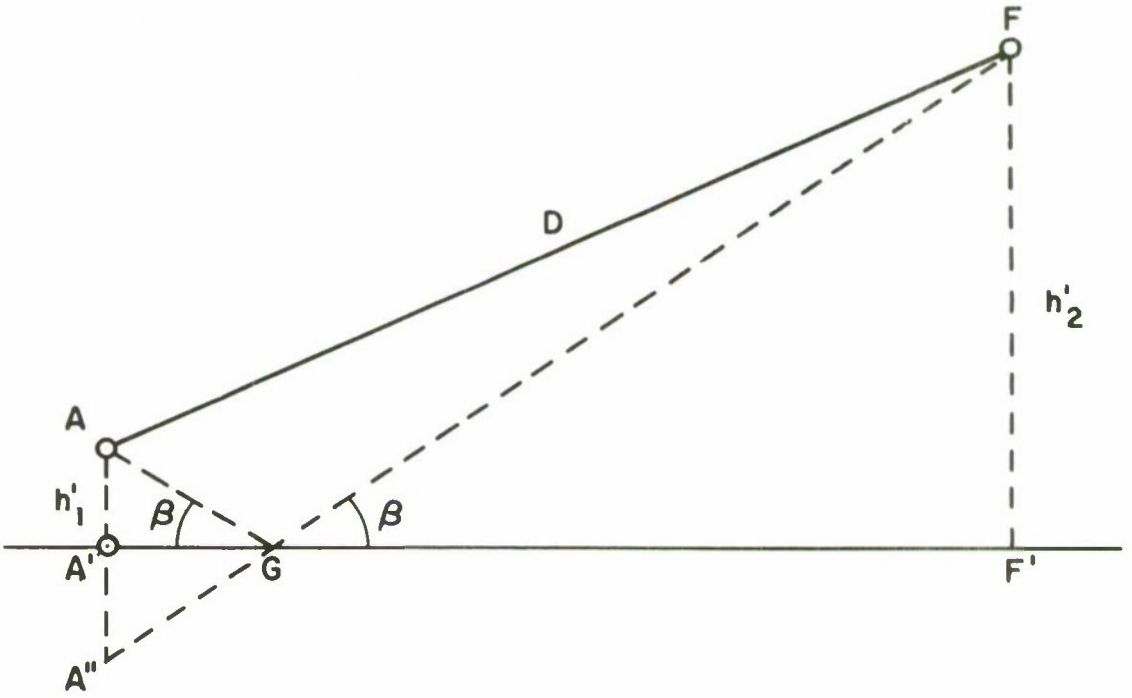

FIGURE 11 FLAT EARTH REFLECTION GEOMETRY

A3422

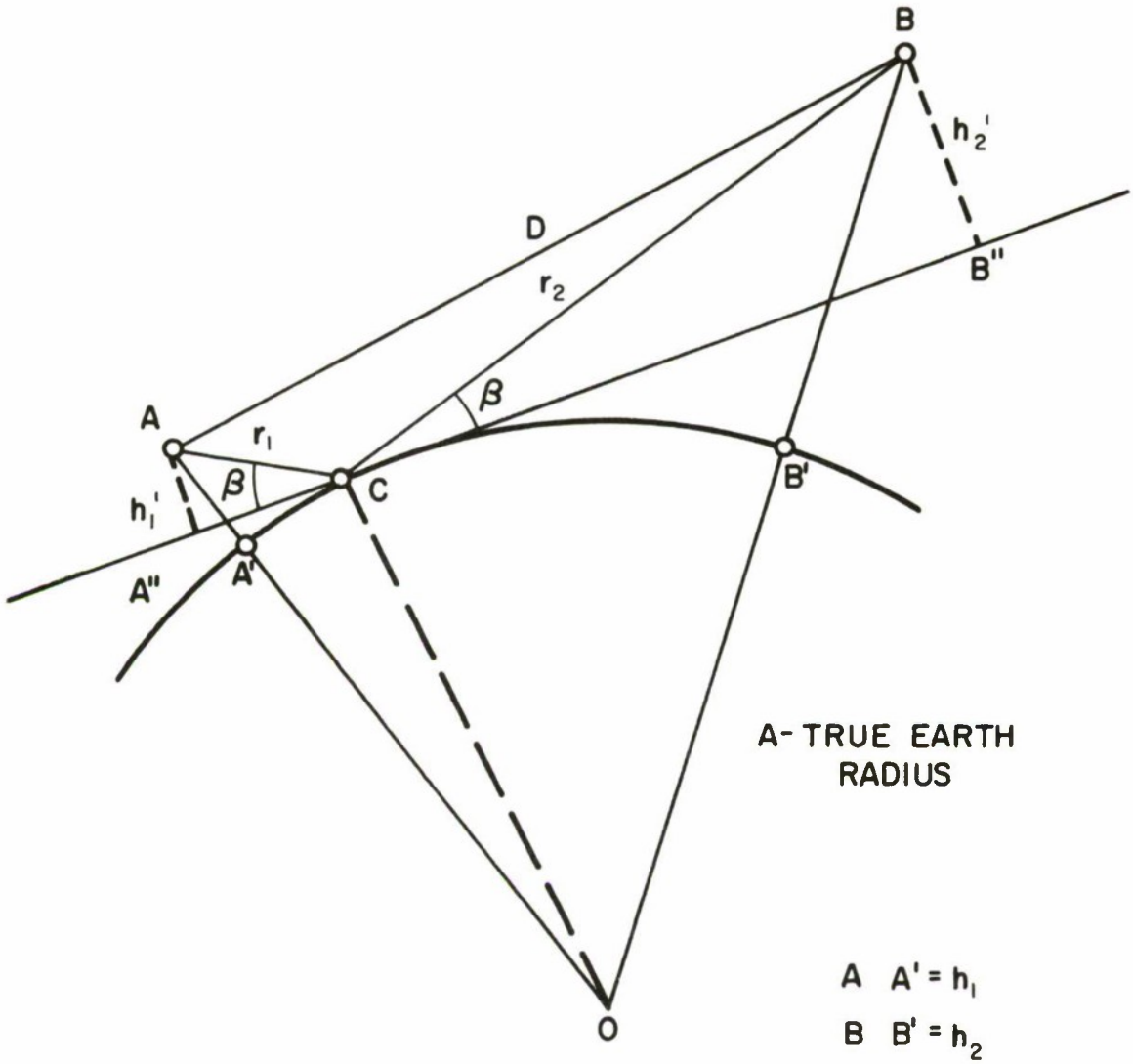

FIGUF 12 GEOMETRY OF FLAT EARTH APPROXIMATION

Therefore

$$h_2' \simeq h_2 - \frac{r_2^2}{2A} \tag{I-5}$$

similarily it can be shown that

$$h_1' \simeq h_1 - \frac{r_1^2}{2A} \tag{I-6}$$

Substituting these equations into Equation (I-1) gives

$$D_n \simeq \frac{2\left(h_1 - \frac{r_1^2}{2A}\right)\left(h_2 - \frac{r_2^2}{2A}\right)}{n\lambda} \tag{I-7}$$

Since the angles of incidence and reflection are equal, we have

$$\frac{r_1}{h_1 - \frac{r_1^2}{2A}} = \frac{r_2}{h_2 - \frac{r_2^2}{2A}} \tag{I-8}$$

However, at any particular fade, of order n, we have

$$(r_1 + r_2) - D_n = n\lambda \tag{I-9}$$

or $$r_2 = D_n - r_1 + n\lambda \tag{I-10}$$

Over the range of experimental interest, $n\lambda$ will be less than about 20 feet ($n \leq 50$ for $\lambda \sim 10$ cm and $n \leq 20$ for $\lambda \sim 30$ cm) and r_1 will be greater than 10 miles. Therefore Equation (I-10) is approximately

$$r_2 \simeq D_n - r_1 \tag{I-11}$$

Substituting into Equation (I-7) and (I-8) gives

$$D_n \simeq \frac{2\left(h_1 - \frac{r_1^2}{2A}\right)\left(h_2 - \frac{(D_n - r_1)^2}{2A}\right)}{n\lambda} \tag{I-12}$$

and $$\frac{r_1}{h_1 - \frac{r_1^2}{2A}} = \frac{D_n - r_1}{h_2 - \frac{(D_n - r_1)^2}{2A}} \tag{I-13}$$

Finally from triangle AA"C and Equation (I-6)

$$\sin \beta \simeq \frac{h_1 - \frac{r_1^2}{2A}}{r_1} \qquad \text{(I-14)}$$

Under propagation conditions in the real atmosphere, of course, the range D_n to the transmitter is a curved path rather than a straight line. However, if a straight path range D_n is assumed, and the terminal heights h_1 and h_2 retained in magnitude, the geometry as shown in Figure 12 will simply give a value of the earth's radius Ae which is larger than the true earth radius A. The above equations are therefore quite general and, by substituting Ae for A, they can be used to generate values of the effective earth's radii.[1] A 7094 computer program was used to solve the above equations for the particular, known input parameters λ, n, D_n, h_1, and h_2 involved in this experiment. From the resulting tables the appropriate values for Ae can be selected, corresponding to the experimental conditions at any particular fade of order n.

APPENDIX II

INTERFEROMETER ERROR ANALYSIS

INTERFEROMETER ERROR ANALYSIS

The error introduced in the Ae calculations can be determined based on the experimental accuracies of D_n, λ, h_1, and h_2. To simplify this analysis, an approximate relationship between these parameters can be determined from the geometry of Figure 13. This geometry was not used for Ae calculations (Reference Appendix I) because it is slightly less accurate and does not give all the parameters required in the overall analysis such as β, r_1 and r_2. Under the range of experimental conditions of interest it may be assumed that the reflection point is very near the receiving terminal and the earth is essentially flat within this confined area. Therefore the flat earth Equation (I-1) can be applied. From Figure 13, it can be shown that

$$h_2' = h_2 \frac{2A + h_2}{2(A + h_1)} - \frac{D_n^2}{2(A + h_1)} + \frac{h_1^2}{2(A + h_1)} \tag{II-1}$$

and for $h_1 << A$ and $h_2 << A$ Equation (II-1) becomes

$$h_2' \simeq h_2 - \frac{D_n^2}{2A} \tag{II-2}$$

Substituting this equation into (I-1), which becomes

$$D_n \simeq \frac{2h_1 h_2'}{n\lambda}$$

(since $h_1' = h_1$), we find that

$$A \simeq \frac{D_n^2 h_1}{2h_1 h_2 - n\lambda D_n} \tag{II-3}$$

Again, this equation is general and A can be replaced by Ae to obtain the dependence of Ae on the parameters measured and applied in the interferometer analysis. Then,

$$\log Ae = 2 \log D_n + \log h_1 - \log (2h_1 h_2 - n\lambda D_n) \tag{II-4}$$

The effect of errors in each of the separate parameters D_n, h_1, h_2, and λ can be found by differentiating Equation (II-4) to give

$$\left(\frac{\delta Ae}{Ae}\right)_{D_n} = \left(\frac{2}{D_n} + \frac{n\lambda}{2h_1 h_2 - n\lambda D_n}\right) \delta D_n \tag{II-5}$$

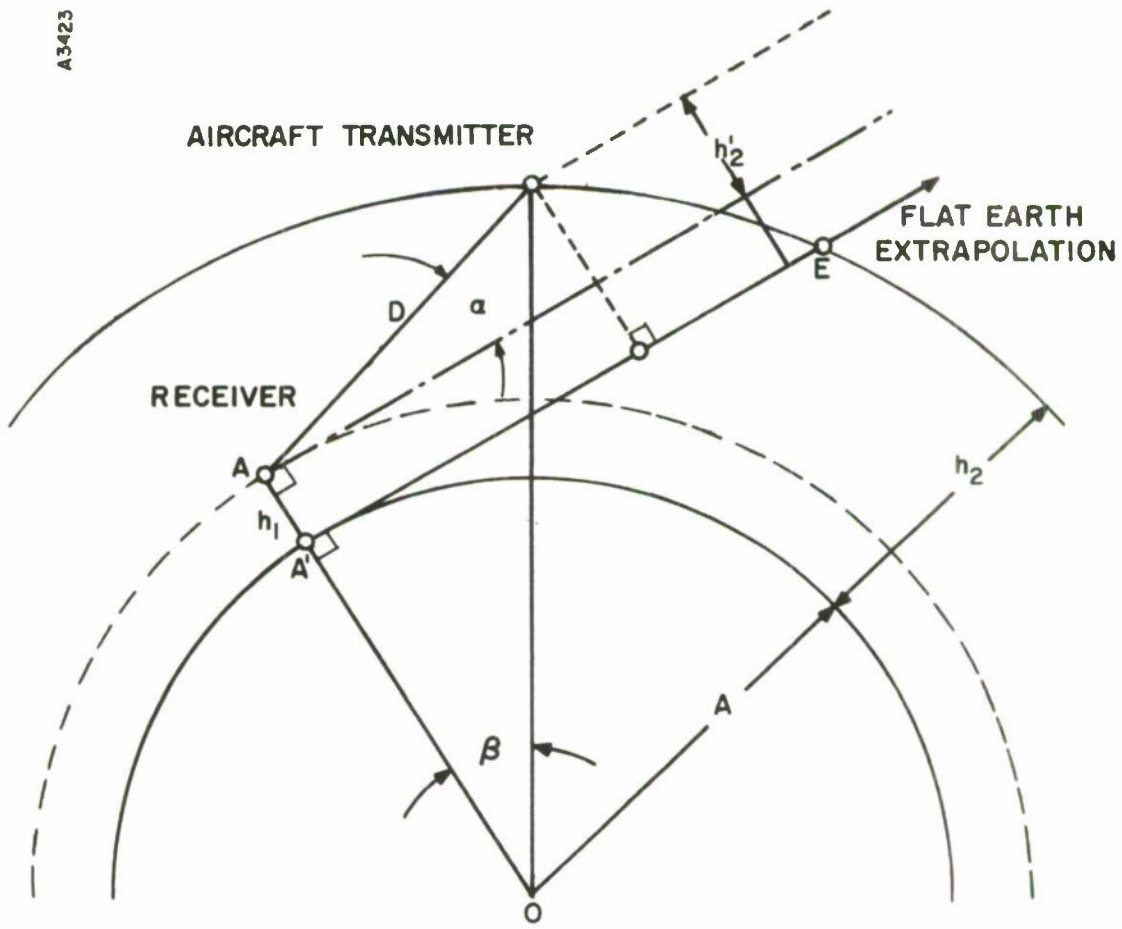

FIGURE 13 GEOMETRY OF FLAT EARTH APPROXIMATION

$$\left(\frac{\delta Ae}{Ae}\right)_{h_1} = \left(\frac{1}{h_1} + \frac{2h_2}{2h_1h_2 - n\lambda D_n}\right) \delta h_1 \qquad \text{(II-6)}$$

$$\left(\frac{\delta Ae}{Ae}\right)_{h_2} = \left(\frac{2h_1}{2h_1h_2 - n\lambda D_n}\right) \delta h_2 \qquad \text{(II-7)}$$

$$\left(\frac{\delta Ae}{Ae}\right)_{\lambda} = \left(\frac{nD_n}{2h_1h_2 - n\lambda D_n}\right) \delta\lambda \qquad \text{(II-8)}$$

From Equation (II-3)

$$2h_1h_2 - n\lambda D_n \simeq \frac{D_n{}^2 h_1}{A} \qquad \text{(II-9)}$$

Substituting this equation into the above gives

$$\left(\frac{\delta Ae}{Ae}\right)_{D_n} = \left(2 + \frac{n\lambda Ae}{h_1 D_n}\right) \frac{\delta D_n}{D_n} \qquad \text{(II-10)}$$

$$\left(\frac{\delta Ae}{Ae}\right)_{h_1} = \left(1 - \frac{2h_2 Ae}{D_n{}^2}\right) \frac{\delta h_1}{h_1} \qquad \text{(II-11)}$$

$$\left(\frac{\delta Ae}{Ae}\right)_{h_2} = \left(\frac{2h_2 Ae}{D_n{}^2}\right) \frac{\delta h_2}{h_2} \qquad \text{(II-12)}$$

$$\left(\frac{\delta Ae}{Ae}\right)_{\lambda} = \left(\frac{n\lambda Ae}{h_1 D_n}\right) \frac{\delta\lambda}{\lambda} \qquad \text{(II-13)}$$

Table II-1 shows the individual errors in $\delta Ae/Ae$ for various test conditions and the total error equivalent to the sum of the individual errors. Finally, multiplying this total error by average earth radii conditions gives the estimated maximum errors in the Ae calculations. A graph of this error relationship to transmitter range is shown in Figure 4.

TABLE II-1
INTERFEROMETER ACCURACY FOR Ae DETERMINATION

n	D_n	Freq. Band	TX Height	$\left(\frac{\delta Ae}{Ae}\right)_\lambda$ $\times 10^{-3}$	$\left(\frac{\delta Ae}{Ae}\right)_{D_n}$ $\times 10^{-3}$	$\left(\frac{\delta Ae}{Ae}\right)_{h_2}$ $\times 10^{-3}$	$\left(\frac{\delta Ae}{Ae}\right)_{h_1}$ $\times 10^{-3}$	Total Error $\times 10^{-3}$	Maximum Error in Ae nm
1	57.0	L	4300	1.26	0.84	10.89	1.22	11	47
3	33.0	L	4300	6.51	3.31	32.45	6.43	33	142
5	22.0	L	4300	16.28	10.18	73.09	16.23	74	318
10	11.0	L	4300	65.13	72.49	292.40	69.11	300	1290
1	77.0	L	7000	0.30	0.57	5.97	0.94	6	26
3	49.0	L	7000	4.39	1.72	14.73	4.38	15	65
5	34.0	L	7000	10.53	4.60	30.60	10.61	31	133
10	19.0	L	7000	37.70	25.03	98.01	37.07	100	430
1	88.0	L	8600	0.81	0.48	4.56	0.80	5	22
3	58.0	L	8600	3.71	1.32	10.51	3.67	11	47
5	41.0	L	8600	8.74	3.30	21.04	8.75	24.6	108
10	23.0	L	8600	31.15	17.33	66.87	13.85	81.8	353
1	69.0	S	4300	1.04	0.55	7.43	0.94	7.7	32
5	41.0	S	4300	8.74	1.89	21.04	8.87	24.5	105
10	25.0	S	4300	28.66	6.88	56.60	29.61	70.3	302
15	18.0	S	4300	59.71	17.94	109.20	60.27	139.4	600
1	90.0	S	7000	0.79	0.41	4.37	0.75	4.5	19
5	60.0	S	7000	5.97	1.03	9.83	5.94	13.0	56
10	39.0	S	7000	18.37	3.13	23.26	18.69	35.2	151
15	29.0	S	7000	37.06	7.54	42.07	36.53	67.3	289
1	102.0	S	8600	0.70	0.36	3.40	0.57	3.5	15
5	70.0	S	8600	5.12	0.83	7.22	5.03	10.2	44
10	47.0	S	8600	15.24	2.28	16.71	16.10	27.9	120
15	34.0	S	8600	31.61	5.48	30.60	32.29	54.8	236

REFERENCES

1. Schelleng, J. C., Burrows, C. R., and Ferrel, E. B., Ultra Short-wave Propagation, Proc. IRE 21, 427-463, March 1933.

2. Starkey, B. J., Rowlandson, L. G., and F/L Fatum, G. A., June 1967, Cold Lake Radio Propagation and Meteorological Experiment - Description of a Radio Meteorological Experiment to Measure Ray Path Bending in the Troposphere With a Vertical Interferometer, The Mitre Corporation, Bedford, Massachusetts, MTR 118, Volume I.

3. Bean, B. R., and Dutton, E. J., Radio Meteorology, National Bureau of Standards Monograph 92, U. S. Government Printing Office, Washington, D. C., 1 March 1966.

UNCLASSIFIED

Security Classification

DOCUMENT CONTROL DATA - R & D

(Security classification of title, body of abstract and indexing annotation must be entered when the overall report is classified)

1. ORIGINATING ACTIVITY *(Corporate author)*
Syracuse University Research Corporation
Applied Sciences Division, Systems Synthesis Laboratory
Merrill Lane, University Heights, Syracuse, New York

2a. REPORT SECURITY CLASSIFICATION
UNCLASSIFIED

2b. GROUP
N/A

3. REPORT TITLE
A METHOD TO DETERMINE AN EFFECTIVE RADIO REFRACTIVITY PROFILE BY DIRECT RADIOMETRIC MEASUREMENTS

4. DESCRIPTIVE NOTES *(Type of report and inclusive dates)*
None

5. AUTHOR(S) *(First name, middle initial, last name)*
Lyall G. Rowlandson

6. REPORT DATE	7a. TOTAL NO. OF PAGES	7b. NO. OF REFS
30 January 1968		

8a. CONTRACT OR GRANT NO.	9a. ORIGINATOR'S REPORT NUMBER(S)
F19628-68-C-0209	ESD-TR-68-307
b. PROJECT NO.	
c.	9b. OTHER REPORT NO(S) *(Any other numbers that may be assigned this report)*
d.	

10. DISTRIBUTION STATEMENT
This document has been approved for public release and sale; its distribution is unlimited.

11. SUPPLEMENTARY NOTES	12. SPONSORING MILITARY ACTIVITY
	Aerospace Instrumentation Program Office, Electronic Systems Division, AFSC, USAF, L G Hanscom Field, Bedford, Mass. 01730

13. ABSTRACT

A vertical reflection interferometer may be used to record the signal received from an airborne source. As the source rises in height a multipath fading pattern is produced. At each ordered fade the experimental geometry can be used to determine a value for an effective earth radius. It is shown that each value of earth radius can be related to an effective refractivity gradient with height from which the refractivity profile can be constructed.

The experimental procedure is based on the results of a comprehensive radio propagation experiment performed at Cold Lake, Alberta, from which it was determined that the effective earth radii could be measured to ±200 nm average using radiometric methods only.

DD FORM 1 NOV 65 1473

UNCLASSIFIED

Security Classification

14 KEY WORDS	LINK A		LINK B		LINK C	
	ROLE	WT	ROLE	WT	ROLE	WT
Effective Earth Radius						
Vertical Interferometer						
Tropospheric Radio Wave						
Multipath Interference						